Effect of the Formation of the Dry Zone Around Underground Power Cables on Their Ratings

Ossama E. Gouda, Adel Z. El Dein, and Ghada M. Amer

***Abstract*—Many factors affect the loading of the underground power cables, such as ambient temperature, depth of laying of cable, number of parallel circuits of cable, and thermal resistivity of the surrounding soil. One important factor, usually ignored, is the formation of dry zones around the underground power cables. Dry zones are usually formed around underground power cables under loading conditions due to the migration of moisture within the soil. In this paper, the effect of the formation of the dry zone on the ampacity of underground power cables is investigated. The derating factor for the formation of dry zones around underground power cables is suggested and calculated for different types of natural backfill soil. IEC 60287-1-3 is taken as a reference. Experimental work was conducted to study the phenomena of the dry zone as related to different types of soils.**

***Index Terms*—Cable ampacity, de-rating factor, dry zone, temperature distribution.**

I. Introduction

THE current ratings of buried cables are determined by the characteristics of surrounding soils and properties of cable as given in IEC 60287-1-3 [1]. In this standard, the thermal resistivity of the soil varies from 0.5 °C.m/W to 1.2 °C.m/W under loading conditions. This value increases due to the dissipated heat from underground power cables. This may lead to thermal instability of the soil around the underground power cable which may lead to thermal failure of the cable [2], [3]. For this reason, derating factors for the loading of cable with respect to the formation of the dry zone have to be considered during the design of the cable network. Several approaches have been adopted to determine the current ratings of buried cables, based on a constant value for the thermal conductivity of the soil [4]–[7]. Mathematical models were proposed by several groups to study the phenomenon of the dry zones around underground power cables [8]–[14]. F. Donazzi *et al.* described the use of sand, silt, cement, and water as backfill materials to improve the ampacity of the cables [15]. In this paper, derating factors for underground power cables, taking into account the formation of the dry zone, are calculated, depending on IEC 60287-1-3 [1]. This paper also describes the phenomena of the formation of the dry zone as related to different types of soil, when these types of soil are subjected to a heat source that simulates a buried cable.

Manuscript received March 25, 2010; revised April 26, 2010, May 28, 2010, June 23, 2010; accepted July 13, 2010. Date of publication August 26, 2010; date of current version March 25, 2011. Paper no. TPWRD-00215-2010.

O. E. Gouda is with the Department of Electrical Engineering, Cairo University, Cairo, Egypt (e-mail: Dr_gouda@yahoo.com).

A. Z. El Dein is with the Department of Electrical Engineering, High Institute of Energy, South Valley University, Aswan 81528, Egypt (e-mail: azeinm2001@hotmail.com).

G. M. Amer is with the Department of Electrical Engineering, High Institute of Technology, Benha University, Egypt (e-mail: dr_ghada11@hotmail.com).

Color versions of one or more of the figures in this paper are available online at http://ieeexplore.ieee.org.

Digital Object Identifier 10.1109/TPWRD.2010.2060369

TABLE I
CLASSIFICATIONS OF THE SIX TYPES OF SOIL

Type of the Soil	Percentage of the weight (%)				Classification
	Gravel	Sand	Silt	Clay	
Sand1	1.5	88.5	10	-	Very coarse sand, poor in gravel, moderately poor in silt
Sand2	2	88.5	9.5	-	Moderately fine sand, poor in gravel, moderately poor in silt
Sand3	13	84	3	-	Medium to coarse sand, some gravel and traces of silt
Sand4	8	92	-	-	Medium to coarse sand, some gravel
Silt + Sand	8	60	30	-	Medium to coarse sand, some gravel
Clay + Silt + Sand	3	37	30	30	Medium to coarse sand, some gravel

II. Experimental Study

A. Experimental Model

Experiments were carried out on six types of natural soil to investigate the drying phenomena and the thermal behavior of the soil around power cables under different loading conditions. The classifications of the six types of soil, according to their composition, are given in Table I.

Fig. 1 gives a sketch of the experimental apparatus used in this test. The sample is contained in a plastic cylinder with a diameter of 100 mm. The height of the soil sample is 100 mm. In the top part, a heat flux (heat source) of known magnitude is introduced in a downward direction; this flux is measured by means of a calibrated meter for heat flux.

The bottom of the sample is in contact with a porous slab of sintered Pyrex glass with small pores (the diameter of the pores is 5 mm). This filter plate is glued on to a vessel of transparent plastic material, which is completely filled with water. This vessel is connected to a leveling bottle through a flexible tube; the water level in this bottle functions as an artificial water table. The cylinder, containing the sample, has been sealed off by an O-ring against the surrounding thermal insulation material. By this apparatus, the moisture tension and, thus, water content can be adjusted. A number of thermocouples are distributed

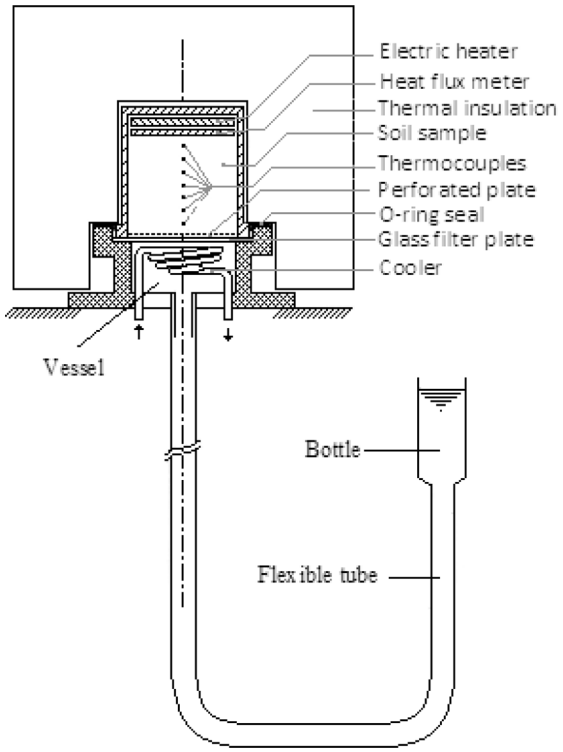

Fig. 1. Apparatus used to simulate the formation of a dry zone around a cable.

from top to bottom of the cylinder to measure the temperature distribution at different points along the sample.

The suction tension is an important factor that affects the thermal soil resistivity and the formation of the dry zones around underground power cables. The moisture retention of soil is controlled by capillarity action. It is described by the moisture potential (α), which is defined as the suction tension of the soil in a water column. This quantity is usually expressed by the associated p_f value which is defined by

$$p_f = \log_{10}(-100\alpha) \tag{1}$$

where p_f represents the logarithm of base 10 of the suction tension. It is true that the suction tension depends on the moisture content, but it also depends more on the history of drying and wetting of the soil. In this paper, the thermal resistivities of the samples are tested at $p_f = \infty$, this is achieved by adjusting the water column to zero.

B. Results of the Experiment

The samples of soil are heated under a heat flux density of 728 W/m^2 and $p_f = \infty$. The temperature distributions at different points along the investigated samples are given separately in figures from 2–7. Common in all figures, there are two slopes for the temperature-distance relationship with respect to time (i.e., there are two zones). Zone1 is formed near the heat source that represents the cable and is known as the dry zone. Zone2 starts from the end of zone1 and is known as the wet zone. The discontinuity in the curves indicates the separation between the dry zone and the wet zone.

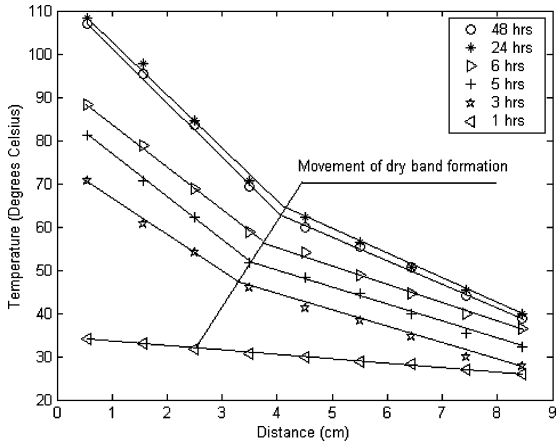

Fig. 2. Temperature versus distance for sand1 when $p_f = \infty$ and $Q_h = 728$ W/m^2.

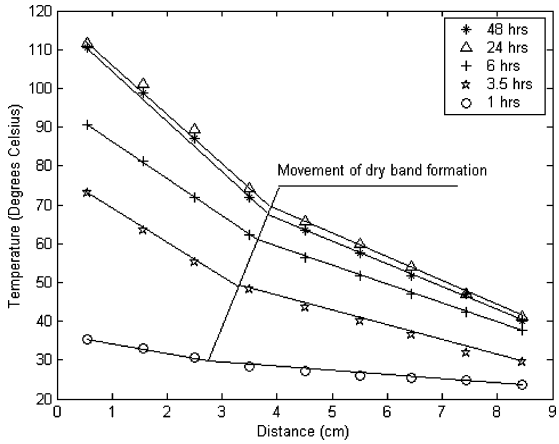

Fig. 3. Temperature versus distance for sand2 when $p_f = \infty$ and $Q_h = 728$ W/m^2.

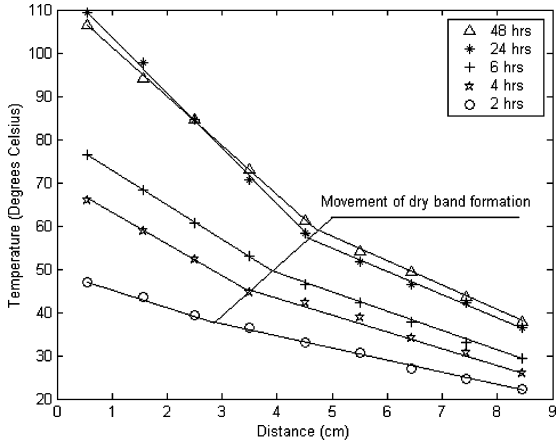

Fig. 4. Temperature versus distance for sand3 when $p_f = \infty$ and $Q_h = 728$ W/m^2.

Interestingly enough, the slope of each zone gives an indication of the increase in the thermal resistivity that could be calculated as follows [1]:

$$\rho = (d\theta/dZ)/Q_h \tag{2}$$

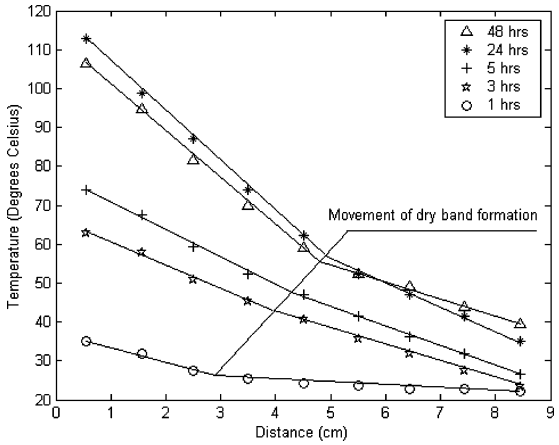

Fig. 5. Temperature versus distance for sand4 when $p_f = \infty$ and $Q_h = 728$ W/m^2.

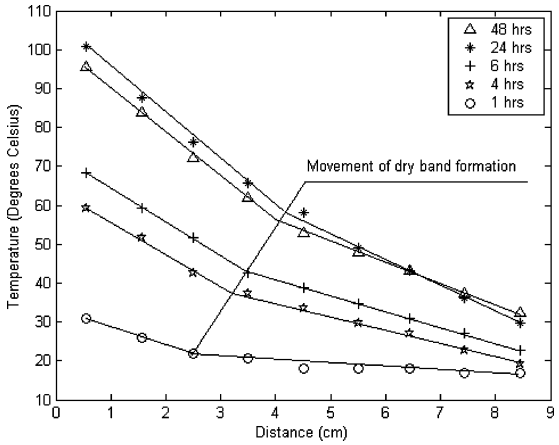

Fig. 6. Temperature versus distance for silt + sand when $p_f = \infty$ and $Q_h = 728$ W/m^2.

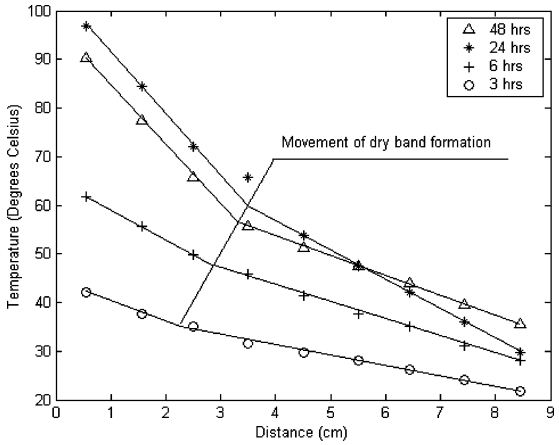

Fig. 7. Temperature versus distance for Clay + Silt + sand when $p_f = \infty$ and $Q_h = 728$ W/m^2.

where

$d\theta/dZ$ temperature gradient (in °C/m);

ρ soil resistivity (in °C.m/W);

Q_h heat flux density (in W/m^2).

TABLE II
THERMAL RESISTIVITY AND THE RATE OF THE FORMATION OF THE DRY ZONE FOR DIFFERENT TYPES OF SOIL

Type of Soil	Q_h W/m^2	p_f	Time in hours	ρ_{dry} °Cm/W	ρ_{wet} °Cm/W	Rate of the formation of the dry zone cm/hrs
Sand1	728	∞	1	0.137	0.137	0.45 between 1 to 3 hours
			3	1.136	0.471	
			5	1.2	0.543	0.1 between 5 to 9 hours
			24	1.67	0.766	0.00416 between 24 to 48 hours
			48	1.64	0.749	
Sand2	728	∞	1	0.188	0.188	0.36 between 1 to 3 hours
			3.5	1.089	0.484	
			6	1.244	0.6	0.016 between 6 to 24 hours
			24	1.648	0.763	0.0041 between 24 to 48 hours
			48	1.737	0.686	
Sand3	728	∞	2	0.549	0.374	0.25 between 2 to 4 hours
			4	0.869	0.549	
			6	1.010	0.597	0.2 between 4 to 6 hours
			24	1.751	0.789	0.033 between 6 to 24 hours
			48	1.537	0.795	0.0085 between 24 to 48 hours
Sand4	728	∞	1	0.477	0.12	0.6 between 1 to 3 hours
			5	0.986	0.670	
			24	1.770	0.784	0.2 between 3 to 5 hours
			48	1.654	0.534	0.0041 between 24 to 48 hours
Silt + Sand	728	∞	1	0.223	0.223	1.66 between 1 to 4 hours
			4	1.098	0.4995	
			6	1.226	0.554	0.15 between 4 to 6 hours
			24	1.590	0.883	0.055 between 6 to 24 hours
			48	1.609	0.732	0.012 between 24 to 48 hours
Clay + Silt + Sand	728	∞	3	0.565	0.283	0.2 between 3 to 6 hours
			6	0.8360	0.481	
			24	1.694	0.824	0.38 between 6 to 24 hours
			48	1.648	0.549	0.01 between 24 to 48 hours

The rate of formation of the dry zone can be calculated by using the following relation:

$$(Z_1 - Z_2)/(t_1 - t_2), \quad \text{where } Z_1 > Z_2 \tag{3}$$

where Z_1 and Z_2 are two positions on the dry zone that are recorded at t_1 and t_2, respectively.

Table II gives the thermal resistivity of different types of soil under testing, when they are loaded by 728 W/m^2 and $p_f = \infty$.

Table II indicates that the dry zone is partially formed after elapsed times of 3 h for sand1, 3.5 h for sand2, 2 h for sand3, 2.7 h for sand4, 4 h for silt + sand, and 3 h for clay + silt + sand. Finally, the dry zones reached steady state after an elapsed time of between 24 to 48 h for the different soils. The results listed in Table II show that the different soils have different thermal resistivities after they are dried. Also, it can be noticed that the rate of formation of the dry zone decreases with time reaching

TABLE III
$(\theta_x - \theta_a)$ AND υ FOR SAMPLES OF SOIL UNDER TESTING

Type of soil	θ_x	θ_a	$v = \frac{\rho_{dry}}{\rho_{wet}}$	θ_x-θ_a
Sand1	63	25	2.179	38
Sand2	65	27	2.16	38
Sand3	58	22	2.21	36
Sand4	56	22	2.257	34
Silt+Sand	57	21	2.1962	38
Clay+Silt+Sand	60	18	2.055	42

a steady state with negligible variation. Some tests were carried out by varying Q_h between 468 W/m^2 and 344 W/m^2, respectively, and it was noticed that the time and the rate of the formation of the dry zone depended on the loading in (W/m^2).

III. Derating Factor Due to the Formation of the Dry Zone

In this paper, the derating factor means the ratio of the current ampacity of the cable calculated upon formation of the dry zone to the current ampacity as calculated by ignoring the formation of a dry zone. IEC 60287-1-3 [1] gives the formula to calculate the current ampacity with respect to the formation of the dry zone. To use this formula, some parameters are needed, such as the ratio between the resistivities of the dry and wet zones of the backfill soil (υ), and the difference between the ambient temperature and the critical temperature of the boundary between the wet and dry zones $(\theta_x - \theta_a)$.

The experimental work carried out in Part 2 of this paper aims to calculate these parameters. These parameters are given in Table III, for the soils under test, when $Q_h = 728$ W/m^2. When the samples of soil are tested by varying Q_h between 468 W/m^2 and 344 W/m^2, respectively, it is noticed that there is little variation in $(\theta_x - \theta_a)$ and in (υ).

Furthermore, from the several tests that were carried out on different soils used as backfill materials, it is noticed that the critical temperature for the formation of the dry zone and the ratio of the thermal resistivity of the dry zone to the resistivity of the wet zone depend on the components of the soil, but are also independent of the loading on the cable. It is interesting to notice that the heat flux, which is produced by underground power cables, is an important factor in determining the time required for the formation of the dry zone. This is in good agreement with F. Donazzi *et al.* [15], [16]. An important conclusion that is derived from the experiment is that both the critical temperature and the ratio of the dry to wet thermal resistivities of the tested soil are independent of the heat flux from the cables. This may be in agreement with Hartley and Black [17], who suggested that the heat flux at the surface of the cable is an important factor in determining the time required for soil to become unstable. From Table III, it is interesting to find that the critical temperatures for moist soils under test are closer to 60 °C rather than the 50 °C that was commonly used by IEC and others [18], [19].

The ampacities of different cables, without and with the effect of the formation of the dry zone taken into consideration, can be calculated by IEC 60287-1-3 according to the equations given in [1]. The current-carrying capacity formula of a buried cable without the effect of the formation of the dry zone is shown in

$$I = \left[\frac{\Delta\theta - W_d\{0.5T_1 + n(T_2 + T_3 + T_4)\}}{R_{\rm ac}\{T_1 + n(1+\lambda_1)T_2 + n(1+\lambda_1+\lambda_2)(T_3+T_4)\}}\right]^{0.5} \tag{4}$$

where

- $\Delta\theta$ — $(\theta_c - \theta_a)$ is the difference between the conductor temperature θ_c and the ambient temperature θ_a°C;
- n — number of load-carrying conductors in the cable (they are of equal size and carry the same load);
- W_d — dielectric loss per unit length for the insulation surrounding the conductor per phase;
- $R_{\rm ac}$ — alternating-current resistance per unit length of the conductor at its maximum operating temperature (Ω/m);
- T_1 — thermal resistance per unit length per core between the conductor and sheath (°C.m/W);
- T_2 — thermal resistance per unit length of bedding between the sheath and armor (°C.m/W);
- T_3 — thermal resistance per unit length of the external serving of the cable (°C.m/W);
- T_4 — thermal resistance per unit length between the cable surface and the surrounding soil (°C.m/W);
- λ_1 — ratio of losses in the metal sheath to total losses in all conductors in that cable;
- λ_2 — ratio of armoring losses to the total losses of conductors in that cable.

The modified formula for rating of a cable, with the effect of the formation of the dry zone taken into consideration, is shown in (5), at the bottom of the page, where

- $\Delta\theta_x$ — $(\theta_x - \theta_a)$, difference between the critical temperature and ambient temperature °C;
- υ — ratio between the thermal resistivities (of dry and wet zones).

Note that $(\theta_x - \theta_a)$ and υ are taken from Table III for different types of soil, and their thermal resistivities are tabulated in Table II. A computer program was used to calculate the derating factor for 11-, 33-, 66-, and 132-kV cables, using the test results for the soils used as backfill materials. Table IV gives a sample of the results. It is concluded that a derating factor due to the formation of a dry zone is between 0.87 and 0.96; and it also

$$I = \left[\frac{\Delta\theta - W_d\{0.5T_1 + n(T_2 + T_3 + \nu T_4)\} + (\nu - 1)\Delta\theta_x}{R_{\rm ac}\{T_1 + n(1+\lambda_1)T_2 + n(1+\lambda_1+\lambda_2)(T_3+\nu T_4)\}}\right]^{0.5} \tag{5}$$

TABLE IV
DERATING FACTOR OF SINGLE-CORE CABLES IN FLAT CONFIGURATION

Type of soil	Sand1	Sand2	Sand3	Sand4	Silt+ sand	Clay+ silt + sand
ρ_{wet} (°C m/W)	0.766	0.763	0.7898	0.784	0.732	0.8341
ρ_{dry} (°C m/W)	1.67	1.648	1.7513	1.77	1.609	1.694
Temperature of the drying zone °C	63	65	58	56	57	60
132 kV cable						
Ampacity without dry zone, Amp.	687	688	678	680	699	666
Ampacity with dry zone. Amp.	643	652	615	609	634	615
De-rating factor	0.935	0.9477	0.9071	0.895	0.907	0.9234
66 kV cable						
Ampacity without dry zone, Amp.	841	842	830	832	858	814
Ampacity with dry zone. Amp.	767	777	734	726	758	734
De-rating factor	0.912	0.9228	0.8843	0.872	0.8834	0.9017
33 kV cable						
Ampacity without dry zone, Amp.	1106	1108	1092	1095	1127	1082
Ampacity with dry zone, Amp.	1024	1037	980	970	1010	979
De-rating factor	0.925	0.9359	0.897	0.8858	0.8962	0.9048
11 kV cable						
Ampacity without dry zone, Amp.	674	675	666	668	686	656
Ampacity with dry zone, Amp.	639	647	613	607	631	612
De-rating factor	0.948	0.9585	0.920	0.908	0.9198	0.9329

depends on the type of backfill and on the rating of the cable. The depth of cables and their spacing are taken as 1 m and 0.4 m, respectively, for cables of voltages higher than 33 kV, and for cables of voltages less than 33 kV, the depth of laying is taken as 0.8 m. The dry zones are formed at 63, 65, 58, 56, 57°C, and 60 °C, respectively, depending on the type of soil. Table IV gives a summary of the calculated results of ampacities of the cables with and without the formation of a dry zone, and gives the de-rating factors for different soils. From the tabulated results, it is clear that sand1 and sand2 have a higher derating factor than the others. They have approximately the same ratio of dry to wet thermal resistivities and the same difference between critical and ambient temperature as given in Table III. They have approximately the same components as given in Table I, but there are little differences in the percentage of weight of gravel and silt. Sand4 has the lowest derating factor, and this can be attributed to the fact that it has the highest value of dry to moist thermal resistivity as given in Table III and because it does not

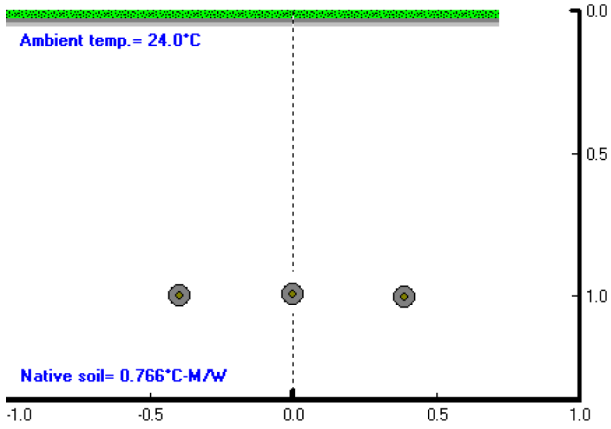

Fig. 8. Geometry of the case study.

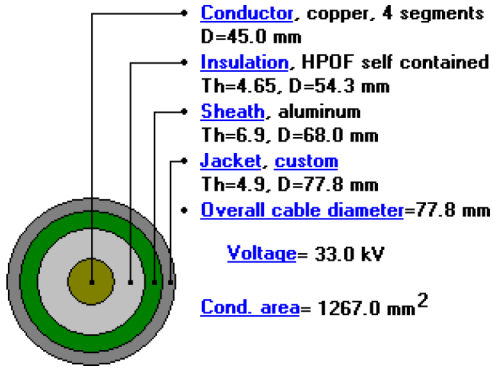

Fig. 9. Details of the construction of the 33-kV single-core cable.

contain any amount of clay or silt. Silt+sand and clay + silt + sand have also good derating factors but they may cause corrosion for a metallic sheath of a cable due to the high amounts of silt that they contain.

IV. TEMPERATURE DISTRIBUTION AROUND UNDERGROUND CABLE

Fig. 8 shows the geometry of the case study, which consists of three single-core cables (33 kV), which form a three-phase circuit that is directly buried in soil of type sand1. The spacing between the adjacent two phases is 0.4 m and the depth of burial is 1 m. The cables are loaded at 1160 A; hence, the maximum temperature of any conductor is fixed at 90 °C. The details of the construction of the cable are given in Fig. 9.

In a system with underground cable, the main heat-transfer mechanism is by conduction. Since the longitudinal dimension of a cable is always much larger than the depth of the installation, the problem becomes a 2-D heat conduction problem. The finite-element method (FEM) is used to study the temperature distribution around the cables. The thermal field in the medium of the cable is governed by the following differential equation [20]–[23]:

$$\frac{\partial}{\partial x}\left[k\frac{\partial \theta}{\partial x}\right]+\frac{\partial}{\partial y}\left[k\frac{\partial \theta}{\partial y}\right]=-q \tag{6}$$

where θ denotes the temperature at any point in the xy plane around the underground cable, k represents the thermal conduc-

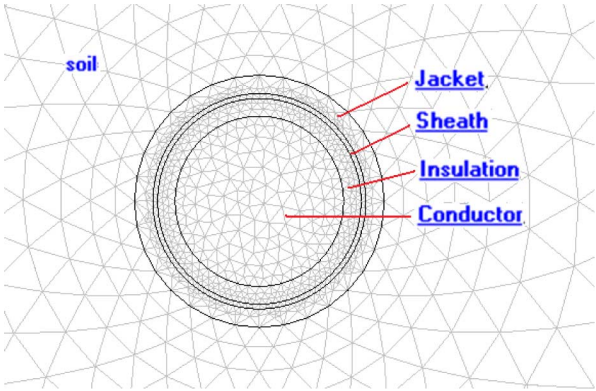

Fig. 10. Sample of finite-element meshes.

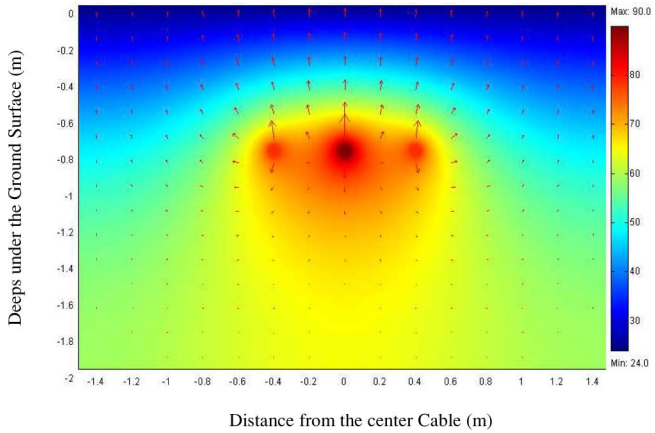

Fig. 11. Distribution of the temperature within and around three single-core cables (33 kV) of flat formation, directly buried in sand1.

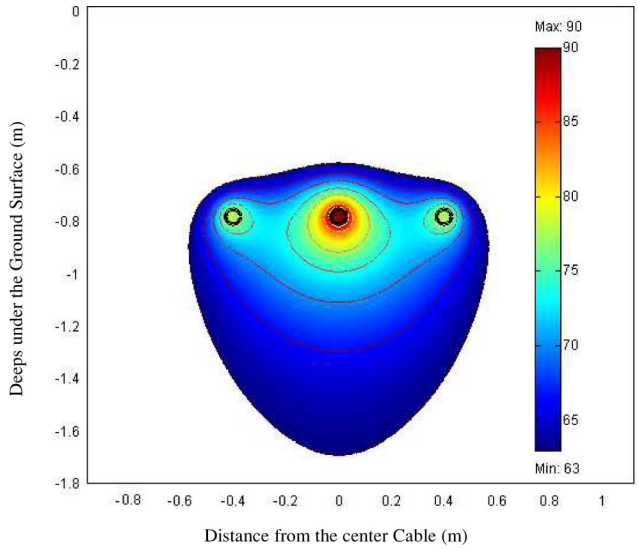

Fig. 12. Formation of the dry zone around three single-core cables (33 kV) of flat formation, directly buried in sand 1.

tivity, q is the heat generation per unit time, and t denotes the time.

For any homogeneous region of a given thermal conductivity and heat generation rate, (6) can be solved for the temperature at any point (x, y) in the region subjected to specified boundary conditions. The thermal circuit of an underground cable includes various regions of complicated shapes having different values of thermal conductivity and heat generation. The FEM exploits the theory that the solution of (6), namely $\theta\ (x, y)$, is the one which minimizes the following function:

$$F = \int\int \left(\frac{1}{2} k \left[\left(\frac{\partial \theta}{\partial x} \right)^2 + \left(\frac{\partial \theta}{\partial y} \right)^2 \right] - q\theta \right) \mathrm{dxdy}. \quad (7)$$

The medium of the cable is partitioned into small elements, normally triangles, forming a mesh as shown in Fig. 10. The minimization of (7) is performed over this mesh yielding a set of linear equations of the following form:

$$H\theta = b \quad (8)$$

where H is the matrix of the heat conductivities, θ is a vector for temperatures at the nodes of the mesh, and b is a vector which normally contains all of the heat generation associated with the node. Both the matrix H and the vector b are adjusted to accommodate the boundary conditions of the thermal circuit [20]–[23]. In this case study, the surface of the soil (upper side in Fig. 8) is represented as an isothermal boundary at ambient temperature and is described by the following equation:

$$\theta = \theta_a \quad (9)$$

where θ_a is the ambient temperature °C. The other three sides have boundaries that are subjected to a specified heat flux condition (i.e., for each boundary side, the divergence of the heat flux in the direction normal to the boundary side is equal to zero) and that is described by the following equation:

$$\frac{\partial \theta}{\partial n} = 0 \quad (10)$$

where n is the outward normal direction to the surface of the boundary side.

Fig. 11 gives the distribution of the temperature around three single-core cables (33 kV) that form a three-phase circuit, as a case study. This circuit is directly buried, at depth of 1 m, in sand1, where the spacing between the adjacent two phases is 0.4 m. Each phase is loaded to 1106 A; hence, the maximum temperature of any conductor is fixed at 90 °C. As is concluded from the experimental results (Table IV), the dry zone can be formed at a critical temperature of 63 °C for sand1. Hence, by drawing the isothermal contour at this critical temperature (in our case study 63 °C), the shape of the dry zone can be detected, which is represented by the area around the three single-core cables, and is closed by the isothermal contour at this critical temperature, as shown in Fig. 12.

V. Conclusion

From the experimental study and the analysis carried out in this paper, it is concluded that:

1) the formation of dry zones around underground cables decreases the capacity of the cables by a factor of 0.87 to 0.96, which is defined in this paper as the derating factor; in addition, this factor depends on the type of soil;

2) from the various tests carried out in this paper, it is observed that the phenomena of the drying zone in backfill started at different temperatures with different velocities depending on the type of soil and the weight percentage of silt;
3) the time required for the formation of the dry zone around buried cables is longer for the sand samples that contain silt than for the samples that do not contain silt; the velocity of the movement of the dry zone around the cables, which are buried in sand that contains silt, is slower than that not containing silt;
4) an important conclusion that is derived from the experimental study is that the critical temperature for wet soils under testing is closer to 60 °C rather than 50 °C that was commonly used by IEC and others [18], [19].

ACKNOWLEDGMENT

The authors would like to thank the reviewers for their constructive comments, which enhanced the material presented in this paper.

REFERENCES

[1] "Calculations of the continuous current rating of cables (100% load factor)." 1982, IEC Publ. 60287-1-3.
[2] G. Koopmans and O. E. Gouda, "Transport of heat and moisture in soils with hysteretic moisture potential," presented at the 4th. Int. Conf. Numerical Methods in Thermal Problems, Swansea, U.K., Jul. 15–18, 1985.
[3] O. E. Gouda, "Formation of the dried out zone around underground cables loaded by peak loadings," in *Modeling, Simulation & Control*. Athens, Greece: ASME Press, 1986, vol. 7, pp. 35–46, No. 3.
[4] J. Hegyi and A. Klestoff, "Current-carrying capability for industrial underground cable installations," *IEEE Trans. Ind. Appl.*, vol. 24, no. 1, pp. 99–105, Jan./Feb. 1988.
[5] M. A. Hanna, A. Y. Chikhani, and M. M. A. Salama, "Thermal analysis of power cables in multi-layered soil- Part 3: Case of two cables in a trench," *IEEE Trans. Power Del.*, vol. 9, no. 1, pp. 572–578, Jan. 1994.
[6] G. J. Anders and H. S. Radhakrishna, "Power cable thermal analysis with consideration of heat and moisture transfer in the soil," *IEEE Trans. Power Del.*, vol. 3, no. 4, pp. 1280–1288, Oct. 1988.
[7] G. J. Anders, A. K. T. Napieralski, and W. Zamojski, "Calculation of the internal thermal resistance and ampacity of 3-core unscreened cables with fillers," *IEEE Trans. Power Del.*, vol. 13, no. 3, pp. 699–705, Jul. 1998.
[8] F. de León and G. J. Anders, "Effects of backfilling on cable ampacity analyzed with the finite element method," *IEEE Trans. Power Del.*, vol. 23, no. 2, pp. 537–543, Apr. 2008.
[9] C. Demoulias, D. P. Labridis, P. S. Dokopoulos, and K. Gouramanis, "Ampacity of low-voltage power cables under non-sinusoidal currents," *IEEE Trans. Power Del.*, vol. 22, no. 1, pp. 584–594, Jan. 2007.
[10] C. Garrido, A. F. Otero, and J. Cidrás, "Theoretical model to calculate steady-state and transient ampacity and temperature in buried cables," *IEEE Trans. Power Del.*, vol. 18, no. 3, pp. 667–678, Jul. 2003.
[11] M. R. Yenchek and G. P. Cole, "Thermal modelling of portable power cables," *IEEE Trans. Ind. Appl.*, vol. 33, no. 1, pp. 72–79, Jan./Feb. 1997.
[12] G. J. Anders, A. Napieralski, and Z. Kulesza, "Calculation of the internal thermal resistance and ampacity of 3-core screened cables with fillers," *IEEE Trans. Power Del.*, vol. 14, no. 3, pp. 729–734, Jul. 1999.
[13] N. P. Schmidt, "Comparison between I.E.E.E. and CIGRE ampacity standards," *IEEE Trans. Power Del.*, vol. 14, no. 4, pp. 1555–1562, Oct. 1999.
[14] G. J. Anders, M. Chaaban, N. Bedard, and R. W. D. Ganton, "New approach to ampacity evaluation of cables in ducts using finite element technique," *IEEE Trans. Power Del.*, vol. PWRD-2, no. 4, pp. 969–975, Oct. 1987.
[15] F. Donazzi, E. Occhini, and A. Seppi, "Soil thermal and hydrological characteristics in designing underground cables," in *Proc. Inst. Elect. Eng.*, Jun. 1979, vol. 126, no. 6.
[16] J. G. Hartley and W. Z. Black, "Transient simultaneous heat and mass transfer in moist unsaturated soils," *ASME Trans.*, vol. 103, pp. 376–382, May 1981.
[17] Anders, *Rating of Electric Power Cables*. New York: IEEE Press/ McGraw-Hill, 1998.
[18] "Determination of a value of critical temperature rise for a cable backfill material," no. 145, pp. 15–30, 1992, CIGRE SC 21, Eletra.
[19] D. S. Freitas, A. T. Prata, and A. J. de Lima, "Thermal performance of underground power cables with constant and cyclic currents in presence of moisture migration in the surrounding soil," *IEEE Trans. Power Del.*, vol. 11, no. 3, pp. 1159–1170, Jul. 1996.
[20] J. H. Neher and M. H. McGrath, "The calculation of the temperature rise and load capability of cable systems," *AIEE Trans.*, vol. 76, pt. 3, pp. 752–772, Oct. 1957.
[21] M. A. El-Kady and O. Hydro, "Calculation of the sensitivity of power cable ampacity to variations of design and environmental parameters," *IEEE Trans. Power App. Syst.*, vol. PAS-103, no. 8, pp. 2043–2050, Aug. 1984.
[22] C. Garrido, A. F. Otero, and J. Cidrás, "Theoretical model to calculate steady-state and transient ampacity and temperature in buried cables," *IEEE Trans. Power Del.*, vol. 18, no. 3, pp. 667–678, Jul. 2003.
[23] M. A. Kellow, "A numerical procedure for the calculation of the temperature rise and apacity of underground cables," *IEEE Trans. Power App. Syst.*, vol. PAS-100, no. 7, pp. 3322–3330, Jul. 1981.

Ossama E. Gouda was born in 1951. He received the B.Sc. degree in electrical engineering in 1975 and the M.Sc. and Ph.D. degrees in high voltage from Cairo University, Cairo, Egypt, in 1979 and 1982, respectively.

From 1988 to 1993, he was Associate Professor, Department of Electrical Engineering, Cairo University. In 1988, he was with the Department of Electrical Engineering, Kema Institute, Arnhem, The Netherlands, where he was a Research Fellow. Since 1993, he has been a Professor in the Electrical Engineering Department, Cairo University, where he is currently the Head of the High Voltage Group of the Electrical Engineering Department. He has published many papers and was supervisor for about 60 M.Sc. and Ph.D. degree candidates. His fields of interest include high-voltage phenomena, protection of power systems, and electromagnetic transients.

Adel Z. El Dein was born in Egypt in 1971. He received the B.Sc. and M.Sc. degrees in electric engineering from the High Institute of Energy, Aswan, Egypt, in 1995 and 2000, respectively, and the Ph.D. degree in electric engineering from Kazan State Technical University, Kazan, Russia, in 2005.

From 1997 to 2002, he was a Teaching Assistant at the High Institute of Energy, Aswan. From 2002 to 2005, he was with Kazan Energy Institute, Kazan, Russia, and Kazan State Technical University. Since 2005, he has been a staff member with the Department of Electrical Engineering, High Institute of Energy. His fields of interest include the calculation of electric and magnetic fields and their effects, comparison of numerical techniques in electromagnetics, design of microstrip antennas and filters, and the calculation of specific absorption rate in the human body.

Ghada M. Amer, photograph and biography not available at the time of publication.